

Optimum Phase Number for Multiphase PWM Inverters

Anwar Muqorobin, Pekik Argo Dahono and Agus Purwadi

School of Electrical Engineering and Informatics, Institute of Technology Bandung
Bandung, Indonesia

anwa006@students.itb.ac.id, pekik@konversi.ee.itb.ac.id and agusp@konversi.ee.itb.ac.id

Abstract—This paper investigates the optimum phase number for multiphase PWM inverters. The input current ripple is used as a performance indicator. Analysis results show that phase number more than nine cannot provide significant input current ripple reduction. Experimental results are included in this paper to show the validity of the proposed analysis method.

Keywords—multiphase; PWM inverters; current ripple.

I. INTRODUCTION

An electric machine with phase number more than three is called multiphase machine. The phase number can be divided into two types, i.e prime phase machine and multiple three-phase machine [1]-[3]. Multiphase machine was firstly attempted to reduce torque pulsation that is inherent in squarewave inverter-fed three-phase machines. The first multiphase machine has shown that five-phase machine could reduce torque pulsation compared to three-phase machine [4]. It was also shown that asymmetrical stator winding configuration is useful to reduce the torque pulsation in multiple three-phase machines [3], [5].

Though torque pulsation is reduced by increasing the phase number, it was shown that stator current ripple is increased. The stator current ripple can be reduced by using appropriate pulselwidth modulation (PWM) techniques. However, this reduction is not significant when the number of phase is more than fifteen [6]-[7]. Another advantages of multiphase machine is torque enhancement when harmonic current injection is used. Compared to three-phase machine with equal size, the torque density of five-phase machine becomes 7.3% higher, for six-phase machine is 7%, seven-phase machine is 1.2% and eleven-phase machine is only 0.2% [8]-[9].

Different to three-phase inverters, just a few works on input current ripple of multiphase PWM inverters have been published. Predetermination of input current ripple is important in selecting input DC filter capacitor. At present, DC filter capacitor is considered as the most unreliable component in power electronic systems. Although various modulation has been proposed to reduce the inverter output current ripple, it has no benefit on the input current ripple [10]-[11]. Further efforts show that the symmetrical configuration gives minimum input current ripple in multiple three phase PWM inverters [12]-[14]. Previous works also have shown that the input current ripple cannot be reduced by increasing the switching frequency but can be reduced by increasing the phase number [10]-[15].

This paper takes further investigation to the maximum phase number that provides significant benefit on the inverter side. This paper concentrates on the analysis of the input current ripple of several multiphase inverters, i.e. from five to seventeen. Experimental results are included to clarify the discussion.

II. INPUT CURRENT RIPPLE ANALYSIS

In this section, input current ripple analysis of inverter-fed six-phase motor is detailed. A similar approach can be applied to other phase numbers. The scheme of inverter-fed six-phase motor is shown in Fig. 1. Two level voltage source inverter is used to drive the motor. A carrier based sinusoidal PWM is used to control the inverter. Sinusoidal reference signals as shown in Fig. 2 are compared to a high frequency triangular carrier signal to produce the ON-OFF signals for the inverter switching devices. If a reference signal is higher than the carrier signal, the associated upper (lower) switching device receives an ON (OFF) signal. For inverter input current ripple analysis, it is assumed that the inverter input voltage is a constant DC voltage with no ripple. Moreover, it is assumed that the inverter switching devices are ideal switches. It is also assumed that the motor is a balanced multiphase motor.

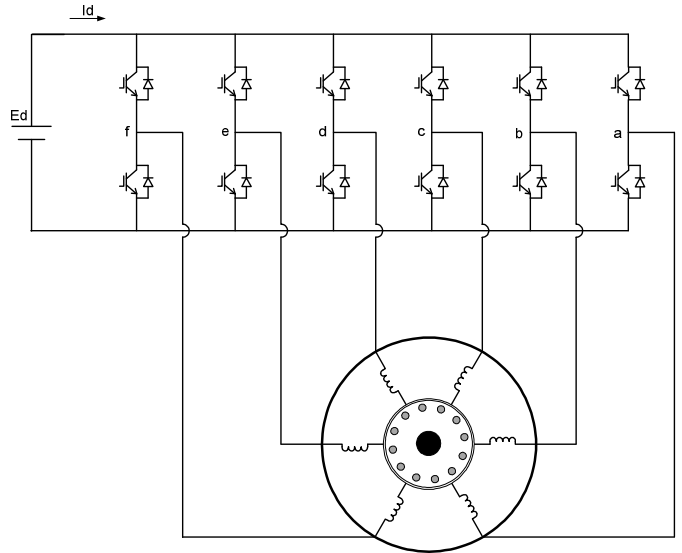


Fig. 1. Six-phase AC drive system.

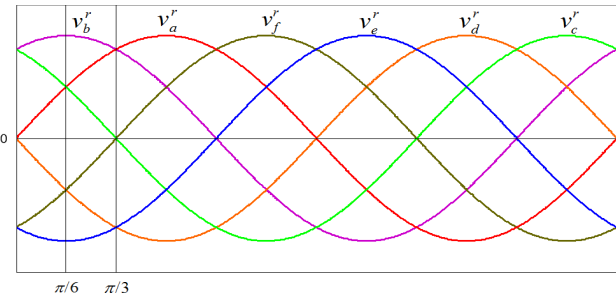


Fig. 2. Reference signals of six-phase inverter.

The sinusoidal reference signals for the inverter are:

$$v_a^r = k \sin(\theta) \quad (1)$$

$$v_b^r = k \sin(\theta + \frac{\pi}{3}) \quad (2)$$

$$v_c^r = k \sin(\theta + \frac{2\pi}{3}) \quad (3)$$

$$v_d^r = k \sin(\theta + \pi) \quad (4)$$

$$v_e^r = k \sin(\theta + \frac{4\pi}{3}) \quad (5)$$

$$v_f^r = k \sin(\theta + \frac{5\pi}{3}) \quad (6)$$

In (1)-(6), v_x^r is the reference signal for phase x , k is modulation index, $\theta = 2\pi ft$, and f is the inverter fundamental frequency.

If the carrier signal frequency is much higher than the fundamental output frequency, the reference signals over one carrier period can be assumed as constants. The inverter waveforms over one carrier period in the interval of $\pi/6$ to $\pi/3$ are shown in Fig. 3.

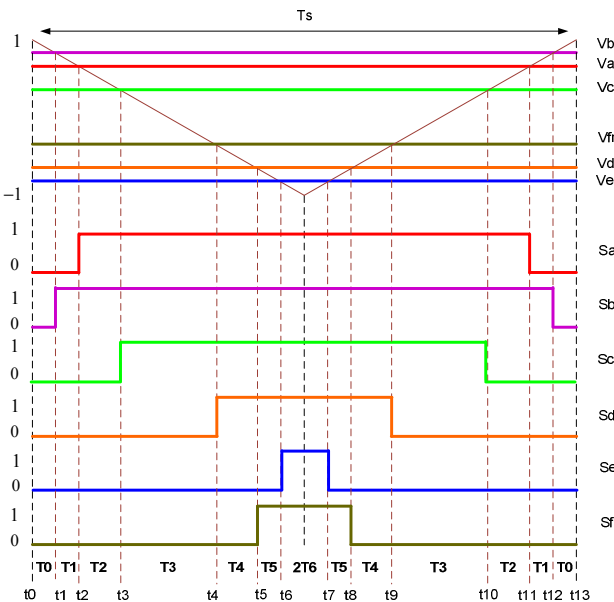


Fig. 3. Detailed waveform during switching periods.

Based on Fig. 3, the time periods can be obtained as in (7)-(13).

$$\frac{T_0}{T_s} = \frac{1-v_b^r}{4} \quad (7)$$

$$\frac{T_1}{T_s} = \frac{v_b^r - v_a^r}{4} \quad (8)$$

$$\frac{T_2}{T_s} = \frac{v_a^r - v_c^r}{4} \quad (9)$$

$$\frac{T_3}{T_s} = \frac{v_c^r - v_f^r}{4} \quad (10)$$

$$\frac{T_4}{T_s} = \frac{v_f^r - v_d^r}{4} \quad (11)$$

$$\frac{T_5}{T_s} = \frac{v_d^r - v_e^r}{4} \quad (12)$$

$$\frac{T_6}{T_s} = \frac{1+v_e^r}{4} \quad (13)$$

When the switching frequency is very high, the output currents can be assumed sinusoidal and can be written as:

$$i_a = \sqrt{2}I_l \sin(\theta - \phi) \quad (14)$$

$$i_b = \sqrt{2}I_l \sin(\theta + \frac{\pi}{3} - \phi) \quad (15)$$

$$i_c = \sqrt{2}I_l \sin(\theta + \frac{2\pi}{3} - \phi) \quad (16)$$

$$i_d = \sqrt{2}I_l \sin(\theta + \pi - \phi) \quad (17)$$

$$i_e = \sqrt{2}I_l \sin(\theta + \frac{4\pi}{3} - \phi) \quad (18)$$

$$i_f = \sqrt{2}I_l \sin(\theta + \frac{5\pi}{3} - \phi) \quad (19)$$

In the above equations, I_l is the rms of output current, ϕ is the power factor angle, and i_x are the output current for phase x .

To calculate the input current ripple, firstly the input current is represented as a function of output currents and the switching function of the inverter as follows.

$$i_d = S_a i_a + S_b i_b + S_c i_c + S_d i_d + S_e i_e + S_f i_f \quad (20)$$

Where S_x equal to unity (zero) when the corresponding upper switching device receives an ON (OFF) signal. The input current during one switching periode in Fig. 3 can be written as shown by (21).

$$i_d = \begin{cases} 0 & , t_0 \leq t \leq t_1 \\ i_b & , t_1 \leq t \leq t_2 \\ i_a + i_b & , t_2 \leq t \leq t_3 \\ i_b - i_e & , t_3 \leq t \leq t_4 \\ -i_d - i_e & , t_4 \leq t \leq t_5 \\ -i_e & , t_5 \leq t \leq t_6 \\ 0 & , t_6 \leq t \leq t_7 \\ -i_e & , t_7 \leq t \leq t_8 \\ -i_d - i_e & , t_8 \leq t \leq t_9 \\ i_b - i_e & , t_9 \leq t \leq t_{10} \\ i_a + i_b & , t_{10} \leq t \leq t_{11} \\ i_b & , t_{11} \leq t \leq t_{12} \\ 0 & , t_{12} \leq t \leq t_{13} \end{cases} \quad (21)$$

The mean square value of the input current in one switching period can be obtained as

$$I_d^2 = \frac{1}{T_s} \int_{t_0}^{T_s+t_0} i_d^2 dt \quad (22)$$

and its average value over one fundamental period is obtained as

$$I_{d,av}^2 = \frac{3}{\pi} \int_0^{\pi} I_d^2 d\theta \quad (23)$$

Finally the mean square value of the input current ripple can be obtained as :

$$\tilde{I}_d^2 = I_{d,av}^2 - \bar{I}_d^2 \quad (24)$$

where

$$\bar{I}_d = \frac{3\sqrt{2}}{2} k \cdot I_l \cdot \cos \phi \quad (25)$$

is the DC component of the input current. The resulted input current ripple of six-phase inverter is

$$\tilde{I}_d^2 = \frac{kI_l^2}{\pi} [\cos^2 \phi (8 + 4\sqrt{3}) - 1 + \sqrt{3}] - \frac{9}{2} k^2 I_l^2 \cos^2 \phi \quad (26)$$

By using the same method, inverter input current ripple of other multiphase inverters can be determined. The results are shown in the Appendix.

III. COMPARISON

Figs. 4 and 5 show the inverter input current ripple as a function of modulation index for power factors of 0.8 and 1.0, respectively. In these figures, the input current ripples of multiphase inverters are normalized with respect to three-phase inverters, with equal total output current. These figures show that under the same total output power, the input current ripple of the inverter is reduced with the increase of phase number. However, this reduction is not proportional to the phase number. A significant reduction is obtained when the phase number is increased from three to five. The reduction is higher when the modulation index is closed to unity.

Fig. 6 shows the normalized input current ripple value when the modulation index is unity for both power factors. The figure shows that the input current ripple reduction is not significant when the phase number is more than nine. The phase number more than nine is suitable in application where another reasons e.g. reliability or power semiconductor rating are considered.

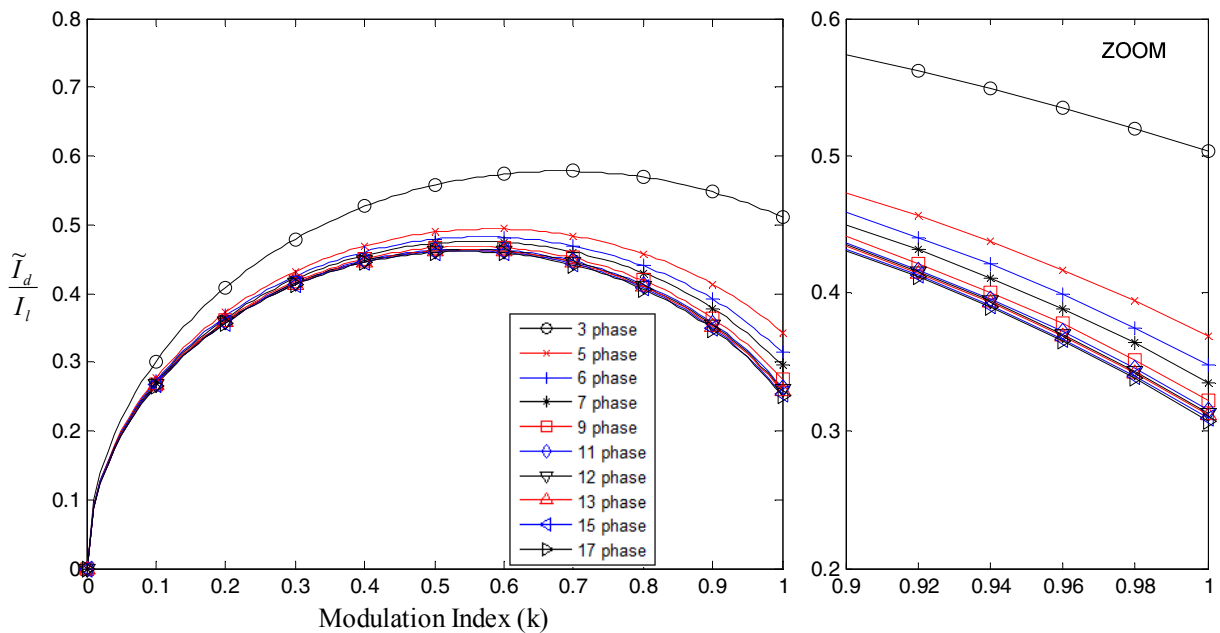


Fig. 4. Input current ripple when PF=0.8.

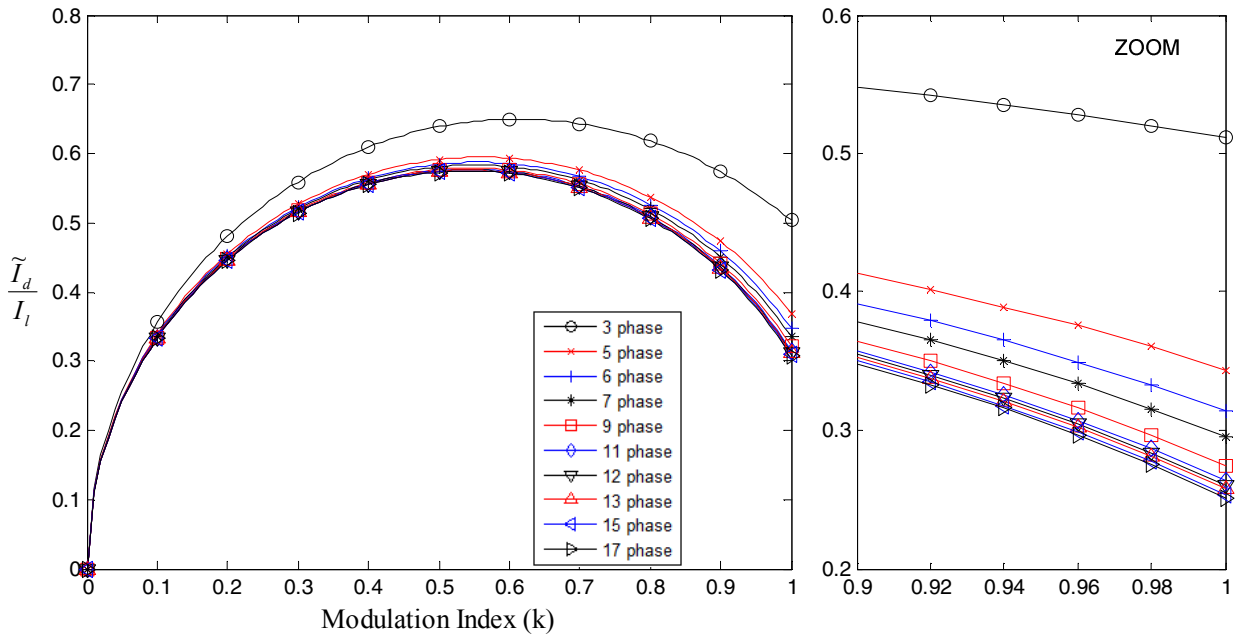


Fig. 5. Input current ripple when PF=1.0.

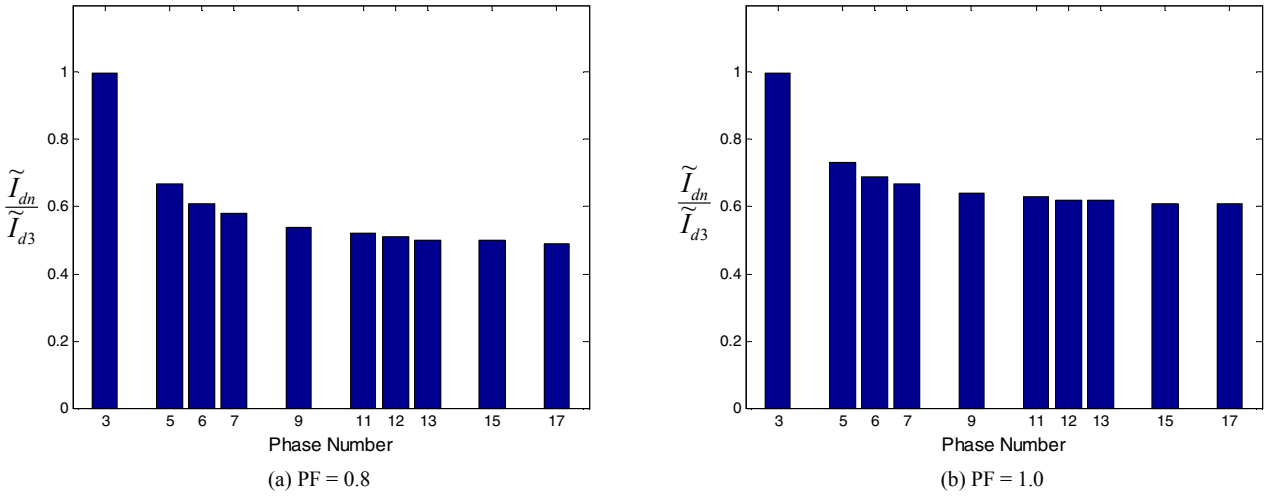


Fig. 6. Input current ripple when modulation index is unity.

IV. EXPERIMENTAL RESULTS

The experiments were carried out using six-phase and nine-phase machines. Both machines are locked during the experiments. The inductance of six-phase machine is 12.52 mH and the resistance is 2.7 Ohm. For the nine-phase machine, the inductance is 10.04 mH and the resistance is 1.78 Ohm. The DC input for the inverters was set to 40 Vdc. The PWM uses carrier frequency of 1 kHz. The input current ripple is measured by using a digital oscilloscope then the results are processed by using a digital computer.

The experimental results are shown in Figs. 7 and 8 for six-phase and nine-phase inverters, respectively. From these

figures, very good agreement between the calculated and experimental results can be appreciated.

V. CONCLUSION

Analysis method for input current ripple of multiphase inverters with phase number of five to seventeen have been presented. It has been shown that the inverter input current ripple can be reduced by increasing the phase number. However, the reduction is not significant when the phase number is more than nine. Experimental results have been included in this paper to verify the proposed analysis method.

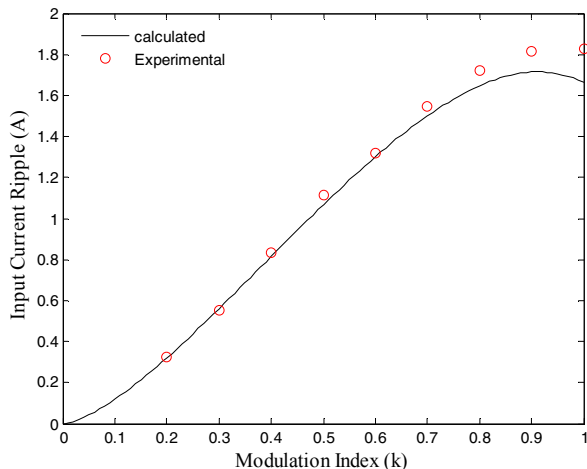


Fig. 7. Input current ripple of six-phase inverter.

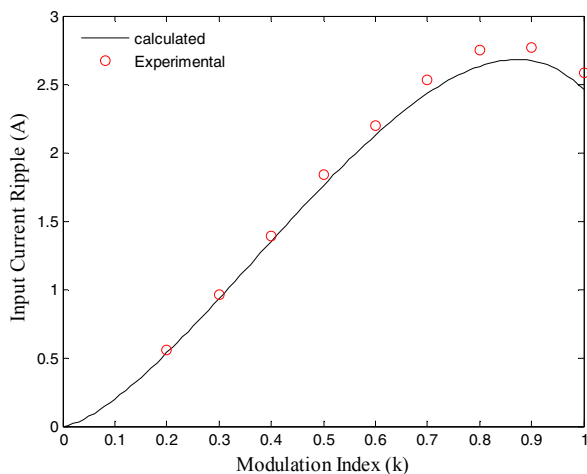


Fig. 8. Input current ripple of nine-phase inverter.

ACKNOWLEDGMENT

The first author thanks to Research Center for Electrical Power and Mechatronics, Indonesian Institute of Sciences (P2 Telimek-LIPI) and Kemenristekdikti Indonesia for doctoral scholarship.

REFERENCES

- [1] H.A. Toliyat, T.A. Lipo, and J.C. White, "Analysis of a concentrated winding induction machine for adjustable speed drive applications part 2 (motor design and performance)," *IEEE Trans. Energy Convers.*, vol. 6, no. 4, pp. 684-692, Dec. 1991.
- [2] E. Levi, R. Bojoi, F. Profumo, H.A. Toliyat, and S. Williamson, "Multiphase induction motor drives—a technology status review," *IET Elect. Power Appl.*, vol. 1, no. 4, pp. 489-516, Jul. 2007.
- [3] E.A. Klingshirn, "High phase order induction motors-part I-description and theoretical considerations," *IEEE Trans. Power App. Syst.*, vol. PAS-102, no. 1, pp. 47-53, Jan. 1983.
- [4] E.E. Ward and H. Harer, "Preliminary investigation of an inverter-fed 5-phase induction motor," *PROC. IEE*, vol. 116, no. 6, pp. 980-984, Jun. 1969.

- [5] R.H. Nelson and P.C. Krause, "Induction machine analysis for arbitrary displacement between multiple winding sets," *IEEE Trans. Power App. Syst.*, vol. PAS-93, no. 3, pp. 841-848, May 1974.
- [6] J. Apsley, S. Williamson, A. Smith, and M. Barnes, "Induction motor performance as a function of phase number," *Electric Power Applications*, vol. 153, no. 6, pp. 898-904, Nov. 2006.
- [7] S. Williamson and S. Smith, "Pulsating torque and losses in multiphase induction machines," *IEEE Trans. Ind. Appl.*, vol. 39, no. 4, pp. 986-993, Jul./Aug. 2003.
- [8] A.S. Abdel-Khalik, M.I. Masoud, S. Ahmed, and A.M. Massoud, "Effect of current harmonic injection on constant rotor volume multiphase induction machine stators: a comparative study," *IEEE Trans. Ind. Appl.*, vol. 48, no. 6, pp. 2002-2013, Nov./Dec. 2012.
- [9] R.O.C. Lyra and T.A. Lipo, "Torque density improvement in a six-phase induction motor with third harmonic current injection," *IEEE Trans. Ind. Appl.*, vol. 38, no. 5, pp. 1351-1360, Sep./Oct. 2002.
- [10] P.A. Dahono, Deni, C.P. Akbarifutra, and A. Rizqianwan, "Input ripple analysis of five-phase pulsewidth modulated inverters," *IET Power Electron.*, vol. 3, no. 5, pp. 716-723, 2010.
- [11] R. Bojoi, M.C. Caponet, G. Grieco, M. Lazzari, A. Tenconi, and F. Profumo, "Computation and measurements of the DC link current in six-phase voltage source PWM inverters for AC motor drives," in *Proc. Power Conversion Conference*, Osaka, 2002, pp. 953-958.
- [12] R.S. Parlindungan and P.A. Dahono, "Input current ripple analysis of double stator AC drive systems," in *International Conference on Information Technology and Electrical Engineering (ICITEE)*, Yogyakarta, 2013, pp. 370-374.
- [13] D. Nurafiat and P.A. Dahono, "Input current ripple analysis of nine-phase PWM inverters," in *37th Annual Conference on IEEE Industrial Electronics Society (IECON)*, Melbourne, 2011, pp. 1378-1383.
- [14] A. Muqorobin and P.A. Dahono, "Optimal displacement for nine phase inverter," in *Proceedings of the Joint International Conference on Electric Vehicular Technology and Industrial, Mechanical, Electrical and Chemical Engineering (ICEVT & IMECE)*, Surakarta, 2015, pp. 258-262.
- [15] M. Lazzari, F. Profumo, A. Tenconi, and G. Grieco, "Analytical and numerical computation of RMS current stress on the DC link capacitor in multiphase voltage source PWM inverters," in *EPE*, Graz, 2001, pp. 1-10.

APPENDIX

Input current ripple of multiphase PWM inverters

Phase number	Input current ripple \tilde{I}_d^2
3	$\frac{kI_l^2}{\pi} \left[2\sqrt{3} \cos^2 \phi + \frac{\sqrt{3}}{2} \right] - \frac{9}{8} k^2 I_l^2 \cos^2 \phi$
5	$\frac{kI_l^2}{\pi} \left[\frac{20}{3} \left(\sin\left(\frac{2\pi}{5}\right) + \sin\left(\frac{\pi}{5}\right) \right) \cos^2 \phi + \frac{10}{3} \left(2 \sin\left(\frac{\pi}{5}\right) - \sin\left(\frac{2\pi}{5}\right) \right) \right] - \frac{25}{8} k^2 I_l^2 \cos^2 \phi$
6	$\frac{kI_l^2}{\pi} \left[\frac{(8+4\sqrt{3}) \cos^2 \phi}{-1+\sqrt{3}} \right] - \frac{9}{2} k^2 I_l^2 \cos^2 \phi$
7	$\frac{kI_l^2}{\pi} \left[\frac{28}{3} \left(\sin\left(\frac{\pi}{7}\right) + \sin\left(\frac{2\pi}{7}\right) + \sin\left(\frac{3\pi}{7}\right) \right) \cos^2 \phi + \frac{14}{3} \left(-\sin\left(\frac{\pi}{7}\right) + 2 \sin\left(\frac{2\pi}{7}\right) - \sin\left(\frac{3\pi}{7}\right) \right) \right] - \frac{49}{8} k^2 I_l^2 \cos^2 \phi$
9	$\frac{kI_l^2}{\pi} \left[\frac{\left(24 \sin\left(\frac{4\pi}{9}\right) + 6\sqrt{3} \right) \cos^2 \phi}{+6 \sin\left(\frac{4\pi}{9}\right) - 3\sqrt{3}} \right] - \frac{81}{8} k^2 I_l^2 \cos^2 \phi$
11	$\frac{kI_l^2}{\pi} \left[\frac{44}{3} \left(\sin\left(\frac{\pi}{11}\right) + \sin\left(\frac{2\pi}{11}\right) + \sin\left(\frac{3\pi}{11}\right) + \sin\left(\frac{4\pi}{11}\right) + \sin\left(\frac{5\pi}{11}\right) \right) \cos^2 \phi + \frac{22}{3} \left(2 \sin\left(\frac{\pi}{11}\right) - \sin\left(\frac{2\pi}{11}\right) - \sin\left(\frac{3\pi}{11}\right) + 2 \sin\left(\frac{4\pi}{11}\right) - \sin\left(\frac{5\pi}{11}\right) \right) \right] - \frac{121}{8} k^2 I_l^2 \cos^2 \phi$
12	$\frac{kI_l^2}{\pi} \left[\frac{(16+8\sqrt{6}+8\sqrt{2}+8\sqrt{3}) \cos^2 \phi}{-2+2\sqrt{6}-4\sqrt{2}+2\sqrt{3}} \right] - 18 k^2 I_l^2 \cos^2 \phi$
13	$\frac{kI_l^2}{\pi} \left[\frac{52}{3} \left(\sin\left(\frac{\pi}{13}\right) + \sin\left(\frac{2\pi}{13}\right) + \sin\left(\frac{3\pi}{13}\right) + \sin\left(\frac{4\pi}{13}\right) + \sin\left(\frac{5\pi}{13}\right) + \sin\left(\frac{6\pi}{13}\right) \right) \cos^2 \phi + \frac{26}{3} \left(-\sin\left(\frac{\pi}{13}\right) + 2 \sin\left(\frac{2\pi}{13}\right) - \sin\left(\frac{3\pi}{13}\right) - \sin\left(\frac{4\pi}{13}\right) + 2 \sin\left(\frac{5\pi}{13}\right) - \sin\left(\frac{6\pi}{13}\right) \right) \right] - \frac{169}{8} k^2 I_l^2 \cos^2 \phi$
15	$\frac{kI_l^2}{\pi} \left[\frac{\left(15\sqrt{3} + 5\sqrt{15} + 10\sqrt{10+2\sqrt{5}} + 5\sqrt{10-2\sqrt{5}} \right) \cos^2 \phi}{+\frac{15}{4}\sqrt{3} + \frac{5}{4}\sqrt{15} - \frac{5}{4}\sqrt{10+2\sqrt{5}} - \frac{5}{2}\sqrt{10-2\sqrt{5}}} \right] - \frac{225}{8} k^2 I_l^2 \cos^2 \phi$
17	$\frac{kI_l^2}{\pi} \left[\frac{68}{3} \left(\sin\left(\frac{\pi}{17}\right) + \sin\left(\frac{2\pi}{17}\right) + \sin\left(\frac{3\pi}{17}\right) + \sin\left(\frac{4\pi}{17}\right) + \sin\left(\frac{5\pi}{17}\right) + \sin\left(\frac{6\pi}{17}\right) + \sin\left(\frac{7\pi}{17}\right) + \sin\left(\frac{8\pi}{17}\right) \right) \cos^2 \phi + \frac{34}{3} \left(2 \sin\left(\frac{\pi}{17}\right) - \sin\left(\frac{2\pi}{17}\right) - \sin\left(\frac{3\pi}{17}\right) + 2 \sin\left(\frac{4\pi}{17}\right) - \sin\left(\frac{5\pi}{17}\right) - \sin\left(\frac{6\pi}{17}\right) + 2 \sin\left(\frac{7\pi}{17}\right) - \sin\left(\frac{8\pi}{17}\right) \right) \right] - \frac{289}{8} k^2 I_l^2 \cos^2 \phi$